Conformation and Thermal Denaturation of Apocalmodulin: Role of Electrostatic Mutations†

Irina Protasevich,‡ Bijan Ranjbar,‡ Vladimir Lobachov,‡ Alexander Makarov,*,‡ Robert Gilli,§ Claudette Briand,§ Daniel Lafitte,|| and Jacques Haiech*,||

Engelhardt Institute of Molecular Biology, Russian Academy of Sciences, Vavilov Street 32, 117984 Moscow, Russia, Faculte de Pharmacie, URA CNRS 1924, Bd Jean Moulin 27, 13385 Marseille Cedex 5, France, and Laboratoire de Chimie Bacterienne, UPR 7221, CNRS, Chemin J. Aiguier 31, 13009 Marseille, France

Received October 9, 1996; Revised Manuscript Received December 3, 1996⊗

ABSTRACT: Scanning microcalorimetry and circular dichroism were used to study conformational state and heat denaturation of Ca^{2+}-free synthetic calmodulin (SynCaM) and three charge reversal mutants. We produced evidence for the major role of the electrostatic potential in the stability and flexibility of SynCaM. The substitution of ^{118}DEE^{120} by ^{118}KKK^{120} (SynCaM12A) does not influence the flexibility of the protein; the replacement of ^{82}EEE^{84} by ^{82}KKK^{84} (SynCaM8) decreases its level, while the combination of these two mutations in SynCaM18A significantly increases the flexibility. The heat denaturation of apoSynCaM and its mutants is well approximated by two two-state transitions with the lower-temperature transition corresponding to C-terminal lobe melting and the higher-temperature one to N-terminal lobe melting. The difference in transition temperatures for the two lobes decreases in SynCaM8 and increases in SynCaM18A, suggesting a modification in the influence of one lobe to the other. The electrostatic mutations change the parameters of thermal denaturation of SynCaM lobes in a similar way as pH conditions affect thermal transition parameters of multidomain proteins, leading to a linear temperature dependence of transition enthalpy. One domain of the N-terminal lobe in apoSynCaM18A is unfolded in the native state. Near-UV CD spectra point out the invariability of the local structure of aromatic residues upon mutations, although the secondary structure undergoes striking transformations. Cacodylate ions strongly and specifically alter the helical content of SynCaM. Our data unambiguously demonstrate that the two lobes are not independent, and interactions between the lobes are mediated by the electrostatic potential of the molecule.

Calmodulin (CaM) is a small (148 residues), acidic, and highly conserved calcium binding protein found in all eukaryotic cells (Kilhoffer et al., 1992a). In order to understand the role of calmodulin in deciphering the calcium signal, it is necessary to analyze the ion binding mechanism of the protein. The apoCaM (Ca^{2+}-free CaM) is the background state and probably plays an important role in the cell. As is known, it can interact, although much more weakly, with some target proteins such as neuromodulin and brush border myosin I (Zhang et al., 1995). It is of paramount importance to describe this state from a structural and thermodynamic point of view.

The three-dimensional crystal structure of Ca^{2+}-CaM was determined at 2.2 Å resolution (Babu et al., 1985) and later was refined at 1.7 Å resolution (Chattopadhyaya et al., 1992). It is a dumbbell-shaped molecule with two roughly globular lobes linked by a long solvent-exposed helix. Each globular lobe contains two Ca^{2+}-binding sites, each consisting of a helix−loop−helix motif (Falke et al., 1994). Studies from different laboratories have shown that the calcium binding to calmodulin is a complex mechanism where coupling between the different sites must take place (Milos et al., 1989; Kilhoffer et al., 1992b; Porumb, 1994). A model considering that the protein is composed of two independent lobes with two cooperative sites (Wang, 1985; Linse et al., 1991) cannot explain all the experimental data. On the other hand, we have shown that coupling exists also between the two lobes of calmodulin during calcium binding (Kilhoffer et al., 1992b).

Before the crystal structure appeared, Tsalkova and Privalov (1985) proposed a domain-melting model for calf brain CaM using the results of the study of thermal unfolding by differential scanning microcalorimetry (DSC). This direct method provides information about the real thermodynamic parameters of thermal transitions in proteins. One of the great advantages of DSC is that it can detect fine tuning of interactions between the individual domains of a protein (Privalov & Potekhin, 1986). Tsalkova and Privalov (1985) have shown that Ca^{2+}-CaM contains four domains, each incorporating one calcium-binding site. The least stable is domain III of the C-terminal lobe which, in the absence of calcium, is in the noncompact disordered state at room temperature. It was shown that the low-temperature peak of apoCaM melting corresponds to the unfolding of domain IV of the C-terminal lobe, and the high-temperature peak comprises the melting of a single cooperative system of the N-terminal lobe (domains I and II). Recently, the three-dimensional structure of CaM in the absence of calcium has been determined by heteronuclear NMR (Kuboniwa et al.,

† This work was supported by INTAS Grant 94-2068.

* To whom correspondence should be addressed. Phone: 33 4 91 16 42 21. Fax: 33 4 91 71 14 89. E-mail: haiech@ir2lcb.cnrs-mrs.fr.

‡ Russian Academy of Sciences.

§ URA CNRS 1924.

|| UPR 7221.

⊗ Abstract published in *Advance ACS Abstracts,* February 1, 1997.

S0006-2960(96)02538-X CCC: $14.00

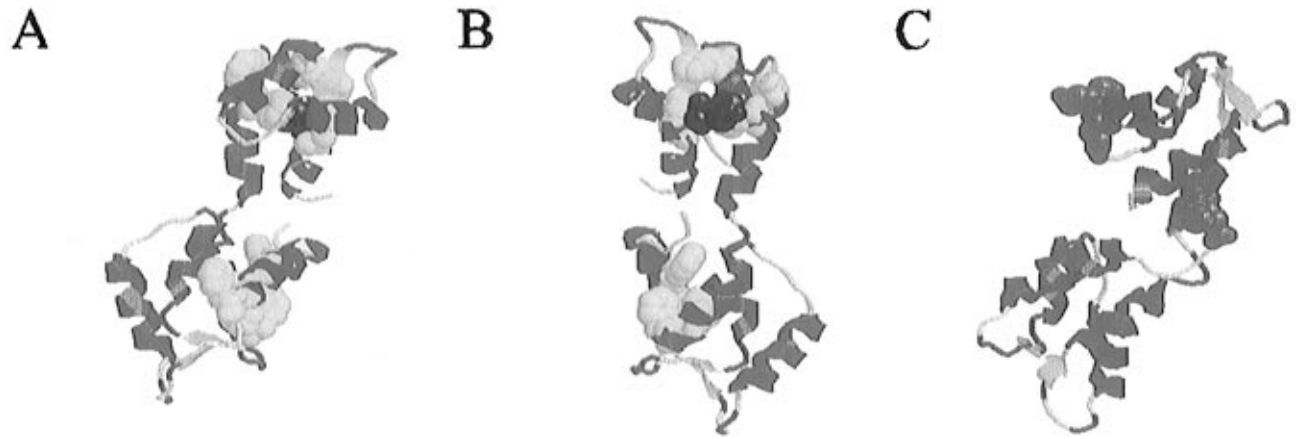

FIGURE 1: Three-dimensional model of apoSynCaM. The coordinates were obtained using ExPASy service (Swiss-Model tools). Template coordinates were taken from set 1CFC in the Brookhaven Protein Data Bank (Kuboniwa et al., 1995). Panels A and B present two different views of apoSynCaM where Phe residues are colored in yellow and Tyr residue in deep blue. Panel C presents a view of apoSynCaM where patches of carboxylic residues that are modified into lysine residues in the different mutants are represented in red.

1995). This study confirms that the C-terminal lobe of apoCaM is considerably less stable than the N-terminal lobe. It was demonstrated that the apocalmodulin backbone must have a nonhelical structure in the C-terminal lobe at least part of the time. Kuboniwa et al. (1995) have proposed that helix F in domain III of the C-terminal lobe is not formed, which qualitatively agrees with a previous calorimetry study of Tsalkova and Privalov (1985).

Studies of calmodulin and various calmodulin-binding model compounds have demonstrated the importance of hydrophobic interactions and charged amino acid residues in calmodulin−peptide or calmodulin−drug complex formation (Afshar et al., 1994). Overall, the data from peptide analogs (binding or enzymatic inhibition) and site-specific mutagenesis suggest an electrostatic component to calmodulin's interaction with macromolecules, including the multiple calmodulin-regulated protein kinases. SynCaM is a synthetic protein hybrid of mammalian and plant CaM able to activate all the Ca^{2+}-calmodulin-dependent enzymes. Its three mutants, SynCaM8, -12A, and -18A, have been designed (Roberts et al., 1985; Craig et al., 1987) to examine the importance of electrostatics in the CaM activation of CaM-dependent enzymes (Craig et al., 1987; Shoemaker et al., 1990; Kosk-Kosicka & Bzdega, 1991; Massom et al., 1991; Farrar et al., 1993). The modifications done on these mutants change the electrostatic potential of the protein in specific parts (clusters of acidic amino acids are replaced by clusters of basic amino acids) and are outside the calcium binding sites (Weber et al., 1989). In SynCaM8, ^{82}EEE^{84} is replaced by ^{82}KKK^{84} in the central helix, and in SynCaM12A, ^{118}DEE^{120} is replaced by ^{118}KKK^{120} in the C-terminal lobe (Figure 1C). SynCaM18A combines these two mutations. The interaction of apoSynCaM and its mutants with calcium was studied by electrospray ionization mass spectrometry (Lafitte et al., 1995), flow dialysis, and isothermal calorimetry (Lafitte et al., 1996). It was shown that the change of electrostatic potential of apoSynCaM has a strong effect on the affinity of all Ca^{2+}-binding sites for calcium. SynCaM8 shows four main binding sites with slightly decreased affinity as compared to those of SynCaM, whereas SynCaM12A and SynCaM18A present, respectively, three and two main sites. However, the influence of this type of mutation on the apoCaM conformation is poorly known. The use of mutants to gain insight into the structure−function relationships requires that a given mutation does not drastically modify the native conformation. The information about conformational potentialities of apoCaM is also essential for a complete understanding of the mechanism of apoCaM's interaction with target proteins. There are strong indications that the amino- and carboxyl-terminal lobes of CaM interact during calcium binding (Kilhoffer et al., 1992b; Pedigo & Shea, 1995a,b), although a two-independent lobes model has been presented (Linse et al., 1991). From this point of view, it is important to probe the existence of such interactions in apoCaM.

In this report, to study the conformational changes which can take place upon electrostatic mutations in calmodulin and the existence of coupling between the two lobes, we analyze the thermodynamic parameters of calorimetric melting and CD spectra of apoSynCaM and its SynCaM8, -12A, and -18A mutants. We demonstrate that the redistribution of charges in the C-terminal lobe and the central helix of apoSynCaM results in essential conformational changes in the N-terminal lobe. Thus, the alteration of the distribution of charges in an apoSynCaM molecule by electrostatic mutations leads to significant changes in its thermodynamic and structural characteristics which depend strongly on the location of the amino acid cluster replaced; that is, the electrostatic potential is an important factor in the stability and flexibility of the molecule and in the influence of apoSynCaM lobes on each other.

MATERIALS AND METHODS

Synthetic calmodulins, SynCaM, and its three mutants (SynCaM8, SynCaM12A, and SynCaM18A) were produced and purified as described previously (Roberts et al., 1985; Craig et al., 1987). The purified proteins have been checked by SDS gel electrophoresis, high-performance capillary electrophoresis, and electrospray ionization mass spectrometry. All the proteins were more than 99% pure. The extinction coefficients of calmodulins were determined by taking the absorption spectrum of a given solution and measuring the protein concentration of the same solution by amino acid composition analysis. Subsequently, the protein concentration was determined spectrophotometrically at 280 nm using the molar extinction coefficient of 1560 M^{-1} cm^{-1} for SynCaM, 2074 M^{-1} cm^{-1} for SynCaM8, 1773 M^{-1} cm^{-1}

for SynCaM12A, and 1839 M^{-1} cm^{-1} for SynCaM18A. For all experiments, ultrapure water (milli-Q apparatus, Millipore Inc.) and acid-washed plasticware were used to minimize calcium contamination. Calcium was removed from proteins by trichloroacetic acid treatment (Haiech et al., 1981). Protein solutions were prepared in 10 and 50 mM sodium cacodylate buffer at pH 7.5.

Scanning microcalorimetric measurements of SynCaMs were carried out on a DASM-4 differential scanning microcalorimeter (NPO Biopribor, Pushchino, Russia) in 0.48 mL cells at a heating rate of 1 K/min. An extra pressure of 1.5 atm was maintained during all DSC runs to prevent possible degassing of the solutions on heating. Protein concentrations varied from 0.9 to 3.5 mg/mL. No concentration dependence of the calmodulin denaturation parameters was observed in this concentration range. The heating curves were corrected for an instrumental baseline obtained by heating the solvent used for protein solution. The reversibility of the unfolding was checked routinely by sample reheating after cooling inside the calorimetric cell (Privalov & Potekhin, 1986). The calorimetric denaturation enthalpy (ΔH_{cal}) and the partial molar heat capacity of the protein (C_p) were determined as described elsewhere (Privalov & Potekhin, 1986), assuming that the molecular mass of SynCaM is 16 628 Da and the partial specific volume is 0.72 cm^3 g^{-1} (Tsalkova & Privalov, 1985). The same value of partial specific volume was adopted for all SynCaM mutants. The partial heat capacity of the polypeptide chain in the unfolded conformation was calculated according to Privalov and Makhatadze (1990), using the known heat capacity values of amino acid residues (Makhatadze & Privalov, 1990) and assuming that in the extended conformation of the polypeptide chain all amino acid residues are exposed to water and contribute additively to the heat capacity of the polypeptide chain. To analyze functions of excess heat capacity, we used the software package SCAL2 developed at the Institute of Protein Research (Pushchino, Russia) (Filimonov et al., 1982, 1993), a modification of a method described by Freire and Biltonen (1978). This software allows for determination of the number of two-state transitions contributing to a complex endotherm. Baselines for the purpose of deconvolution were determined by the straight-line method or by the method of splines using the same software. The calorimetric enthalpy values are accurate within ±8%, and C_p values are accurate within ±1.5 kJ K^{-1} mol^{-1}. The errors in the parameters of individual transitions obtained by deconvolution of complex melting curves did not exceed ±12% for the transition enthalpy and ±1.3 °C for the transition temperature.

The hydropathic indexes of SynCaM lobes were calculated by the method of Kyte and Doolitle (1982) by means of the sequence analysis software PC/GENE (IntelliGenetics). This method systematically evaluates the hydrophilic and hydrophobic tendencies of a polypeptide chain and uses a hydropathy scale in which each amino acid has been assigned a value reflecting its relative hydrophilicity and hydrophobicity.

CD spectra were recorded on a JASCO J-715 spectropolarimeter (Japan) using solutions with protein concentrations varying from 0.15 (far-UV) to 1.6 mg/mL (near-UV). The results were expressed as molar ellipticity, [Θ] (deg cm^2 $dmol^{-1}$), based on a mean amino acid residue weight (MRW) assuming its average weight for calmodulin to be equal to 112.4. The molar ellipticity was determined as $[\Theta]_\lambda = (\theta \times 100\text{MRW})/(cl)$, where c is the protein concentration in milligrams per milliliter, l is the light path length in centimeters, and θ is the measured ellipticity in degrees at a wavelength λ. The instrument was calibrated with (+)-10-camphorsulfonic acid, assuming $[\Theta]_{291} = 7820$ deg cm^2 $dmol^{-1}$ (Schippers & Dekkers, 1981), and with JASCO standard nonhydroscopic ammonium (+)-10-camphorsulfonate, assuming $[\Theta]_{290.5} = 7910$ deg cm^2 $dmol^{-1}$ (Takakuwa et al., 1985). Noise in the data was smoothed using the JASCO J-715 software, including the fast Fourier-transform noise reduction routine which allows enhancement of most noisy spectra without distorting their peak shapes.

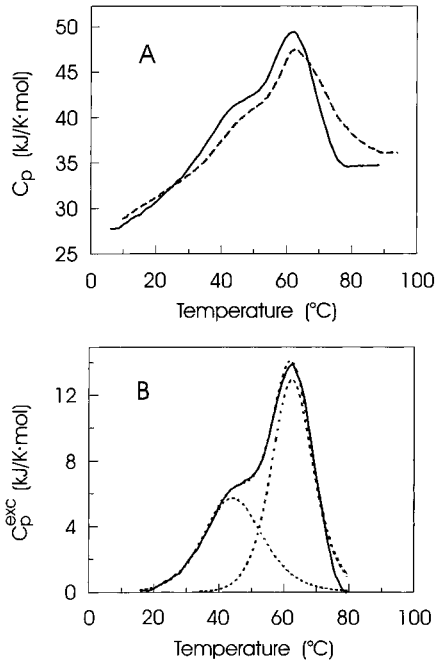

FIGURE 2: (A) Temperature dependence of the partial molar heat capacity of apoSynCaM in 10 mM (dotted line) and 50 mM (solid line) sodium cacodylate buffer at pH 7.5. (B) Computer deconvolution of the transition excess heat capacity of apoSynCaM in 50 mM sodium cacodylate at pH 7.5: experimental results (solid line), deconvoluted peaks, and their sum (dotted lines).

RESULTS AND DISCUSSION

Scanning Calorimetry of apoSynCaM. Figure 2A shows the temperature dependence of the partial molar heat capacity of Ca^{2+}-free SynCaM in 50 and 10 mM sodium cacodylate buffer at pH 7.5. These buffer conditions were choosen as X-ray studies of CaM structure have been done mainly in 50 mM cacodylate buffer, and previous calorimetric investigation of calf brain CaM thermal denaturation was conducted in 10 mM cacodylate buffer (Tsalkova & Privalov, 1985). HEPES that has been mainly used in calcium binding studies was not suitable in our experimental conditions because of an unstable baseline. Both melting curves are asymmetric with a pronounced shoulder at lower temperatures similar to that obtained ealier for calf brain apoCaM (Tsalkova & Privalov, 1985; Hopkins & Gayden, 1990). However, the overall thermostability of apoSynCaM is higher by about 7 °C than that obtained for calf brain apoCaM under the same conditions. Upon the concentration of buffer being decreased from 50 to 10 mM, the heat absorption peak shifts to higher temperatures (Figure 2A). The scanning calorimetric experiments with Ca^{2+}-saturated SynCaM have shown that the melting endotherm was not observed up to 124 °C

Table 1: Scanning Calorimetry Thermodynamic Parameters of Temperature-Induced Denaturation of Calcium Free SynCaM and Its Mutants[a]

protein	C_p^{20} [b] (kJ K^{-1} mol^{-1})	ΔH_{cal} [c] (kJ/mol)	first transition[d] T_t^1 [e] (°C)	first transition[d] ΔH_t^1 [f] (kJ/mol)	second transition[d] T_t^2 [e] (°C)	second transition[d] ΔH_t^2 [f] (kJ/ mol)
10 mM Buffer						
SynCaM	31.4	275	47.7	111	61.2	184
SynCaM8	29.0	267	42.9	107	61.1	183
SynCaM12A	31.5	243	43.4	93	58.5	170
SynCaM18A	38.0	232	40.1	98	65.5	149
50 mM Buffer						
SynCaM	30.6	306	41.2	128	62.0	196
SynCaM8	27.5	320	50.1	136	64.7	200
SynCaM12A	29.5	300	40.0	109	60.0	195
SynCaM18A	35.3	221	34.1	99	62.8	123

[a] Denaturation was performed in sodium cacodylate buffer at pH 7.5. [b] C_p^{20} is the partial molar heat capacity of the protein at 20 °C. Errors are ±1.5 kJ K^{-1} mol^{-1}. [c] Total calorimetric enthalpy of denaturation. Errors are ±8%. [d] Transitions were determined by deconvolution analysis of the heat absorption curves. [e] Errors are ±1.3 °C. [f] Errors are ±12%.

which is near the high-temperature limit of the DASM-4 microcalorimeter. This fact did not allow us to study the influence of mutations on the thermal denaturation parameters of Ca^{2+}-saturated SynCaM.

The partial molar heat capacity of apoSynCaM at 20 °C ($C^{20}{}_p$) is 31.0 ± 1.5 kJ K^{-1} mol^{-1}, does not depend on the buffer molarity, and is close to that of calf brain apoCaM (Tsalkova & Privalov, 1985). This value calculated per gram of protein, 1.9 J K^{-1} g^{-1}, is higher than the average value of the partial specific heat capacity at 20 °C for small globular proteins, 1.3 J K^{-1} g^{-1} (Privalov & Potekhin, 1986). This might be considered an indication that apoSynCaM is more flexible than other small proteins. From X-ray, NMR, and small angle X-ray scattering, it appears that the long central α-helix connecting the two globular lobes is highly flexible in solution (Chazin, 1995; Chattopadhyaya et al., 1992). It is evident that such a structure should give rise to additional flexibility of globular parts relative to each other. According to Privalov and Makhatadze (1990), we have calculated the partial heat capacity of a hypothetical, fully unfolded, and solvent-exposed apoSynCaM from the heat capacities of the individual amino acids, assuming simple additivity. The heat capacity of the denatured apoSynCaM is close to this calculated value which indicates that heat-denatured apoSynCaM is fully unfolded.

The apoSynCaM calorimetric curves are highly reversible on repeated heating of the same sample. The reversibility does not depend on the protein concentration but depends on the temperature to which the protein solution was heated at the first scan. If we stopped heating immediately after the end of the heat absorption peak, the reversibility was practically complete (not less than 95%).

The overall excess heat effect, i.e. the melting enthalpy, ΔH_{cal}, of the apoSynCaM at two buffer concentrations is given in Table 1. The ΔH_{cal} for apoSynCaM is close to that for the calf brain apoCaM (Tsalkova & Privalov, 1985; Hopkins & Gayden, 1990) and slightly changes upon increasing the buffer molarity. The melting curve asymmetry and an extended temperature range of the denaturation process indicate the presence of more than one cooperative transition (Filimonov et al., 1982; Privalov & Potekhin, 1986). Therefore, we carried out a deconvolution of the calorimetric curve for apoSynCaM. The curve can be presented as two overlapping two-state transitions (Figure 2B), similar to that obtained ealier for calf brain apoCaM (Tsalkova & Privalov, 1985). Following Tsalkova and Privalov (1985) and Kuboniwa et al. (1995), the first deconvoluted peak corresponds to C-terminal lobe melting, while the second one is assigned to N-terminal lobe unfolding. The values of hydropathic indexes for N- and C-terminal lobes (−5.0 and −7.4, respectively) calculated on the basis of their primary structure according to Kyte and Doolitle (1982) indicate more hydrophilicity of the C-terminal lobe, i.e. more accessibility for solvent and thus less stability (Privalov & Makhatadze, 1990; Serrano et al., 1993). The maxima of the first and second transition peaks of apoSynCaM (Table 1), as compared with that of calf brain apoCaM, are shifted by 11.7 and 7.2 °C to higher temperatures, respectively. This difference is not surprising since practically all substitutions in the SynCaM amino acid sequence in comparison to those in calf brain CaM are located inside the C-terminal lobe and the central α-helix (Roberts et al., 1985). Moreover, the melting parameters of the low-temperature peak, similar to those of calf brain CaM, are more sensitive to ionic conditions than those of the N-terminal lobe (Table 1). Hence, the structure of the C-terminal lobe should be more sensitive to mutations changing the electrostatic potential of the protein than the N-terminal lobe.

Scanning Calorimetry of ApoSynCaM Mutants. Figure 3 demonstrates the results of calorimetric melting of Ca^{2+}-free SynCaM8, SynCaM12A, and SynCaM18A mutants where clusters of acidic amino acids were replaced by clusters of basic amino acids. All calorimetric curves for mutants are fully reversible on repeated heating of the same sample. The reversibility does not depend on protein concentration but depends on the temperature to which the protein solution was heated at the first scan in the same manner as for apoSynCaM. The curve shapes for mutants differ from that for apoSynCaM. Although the asymmetry of the curves is conserved, the pronounced shoulder in the left part of the melting curve obtained for apoSynCaM decreases significantly. Moreover, the amplitude of the main maximum in case of apoSynCaM18A melting in 50 mM buffer strongly decreases (Figure 3).

The partial molar heat capacity of apoSynCaM12A at 20 °C is close to the corresponding values for apoSynCaM (Table 1). Thus, the substitution of the acidic 118−120 cluster does not influence the flexibility of the protein. The value of C_p^{20} and, consequently, the level of structural flexibility for apoSynCaM8 are the lowest among all calmodulins, while for apoSynCaM18A, they are the highest. The decrease in buffer molarity slightly increases these values for mutants (Figure 3, Table 1).

The heat capacities of the denatured apoSynCaM mutants are close to the values calculated according to Privalov and Makhatadze (1990). Consequently, the heat-denatured mutants, similar to apoSynCaM, are fully unfolded. Thus, the differences in thermodynamic parameters of denaturation for apoSynCaM and its mutants are reflecting the differences in their native states.

The values of denaturation enthalpy of apoSynCaM8 and apoSynCaM12A are near the corresponding values for

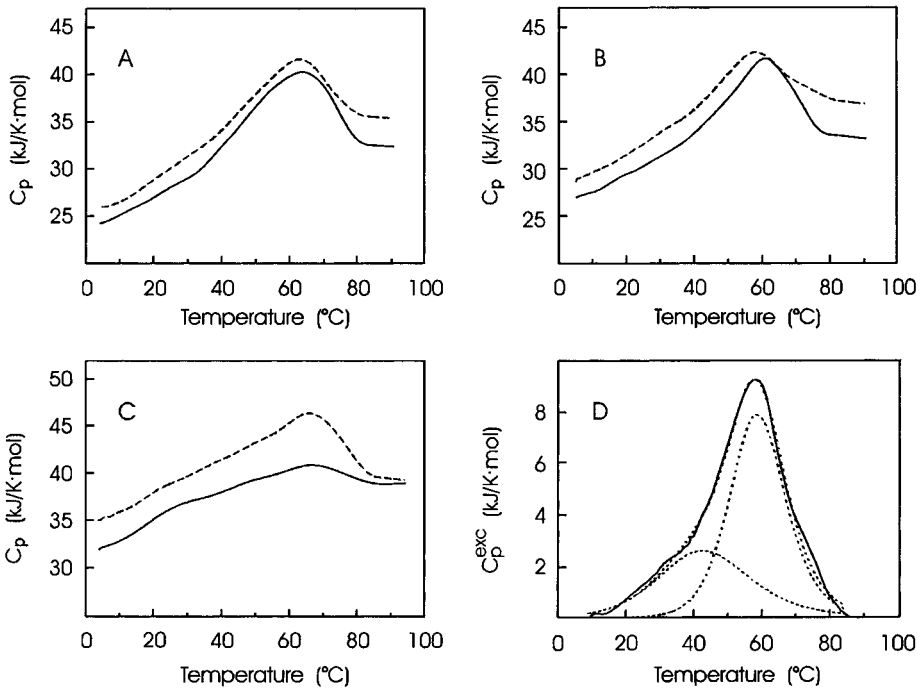

FIGURE 3: Temperature dependence of the partial molar heat capacity of apoSynCaM mutants in 10 mM (dotted line) and 50 mM (solid line) sodium cacodylate buffer at pH 7.5: apoSynCaM8 (A), apoSynCaM12A (B), and apoSynCaM18A (C). (D) Computer deconvolution of the transition excess heat capacity of apoSynCaM12A in 10 mM sodium cacodylate buffer at pH 7.5: experimental results (solid line), deconvoluted peaks, and their sum (dotted lines).

apoSynCaM, while in the case of apoSynCaM18A, they are lower, especially in 50 mM buffer. This indicates that the apoSynCaM18A molecule is less folded than others. The heat denaturation curves for mutants can be deconvoluted, in a manner similar to that for apoSynCaM, into two overlapping two-state transitions (Figure 3D, Table 1). Transition parameters (transition temperature, T_t; transition enthalpy, ΔH_t), especially for the first transition, are different for SynCaM and its mutants. This fact proves the significant role of electrostatic interactions for stabilization of native apoSynCaM structure.

The substitution of acidic cluster 82−84 by the basic cluster in SynCaM (SynCaM8, Table 1, data for 50 mM buffer) leads to the increase of the first transition temperature by 8.9 °C and of the second by 2.7 °C. With the basic cluster in place of acidic cluster 118−120 (SynCaM12A), both the T_t^1 and T_t^2 are slightly lower than those for SynCaM. In the case of SynCaM18A, which combines these two mutations, T_t^1 decreases significantly (by 7 °C) in comparison to that of SynCaM, whereas T_t^2 is equal to that of SynCaM. On the basis of this comparison, we conclude that the effect of the simultaneous substitution of two acidic clusters in SynCaM18A is not the simple sum of the separate effects of each substitution in SynCaM8 and SynCaM12A. Moreover, our data qualitatively agree with the difference of electrostatic energy of stabilization for SynCaM mutants relative to SynCaM computed by Weber et al. (1989).

From this standpoint, we have analyzed the differences in the transition temperatures of the second and the first deconvoluted peaks (ΔT_t, Table 1) for SynCaM and its mutants to estimate the mutation effect on the difference in thermostability of the N- and C-terminal lobes. The substitution of the 118−120 cluster in SynCaM (data for 50 mM buffer) does not influence the difference in thermostability of the lobes (ΔT_t is 20.0 and 20.8 °C for apoSynCaM12A and apoSynCaM, respectively). This value

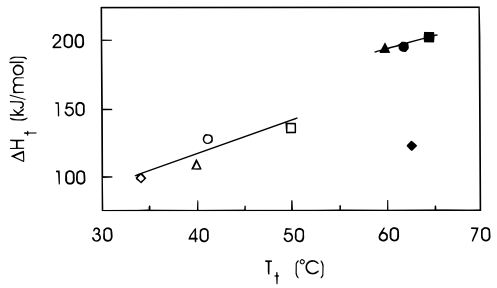

FIGURE 4: Dependence of the denaturation enthalpy on the denaturation temperature for the first (open symbols) and second (filled symbols) deconvoluted peaks of the melting of apoSynCaM and its mutants (50 mM sodium cacodylate buffer at pH 7.5): apoSynCaM (○, ●), apoSynCaM8 (□, ■), apoSynCaM12A (△, ▲), and apoSynCaM18A (◇, ◆).

decreases for apoSynCaM8 (ΔT_t is 14.6 °C) and increases for apoSynCaM18A (ΔT_t is 28.7 °C). Probably, it shows that the influence of the lobes on each other increases in apoSynCaM8 and decreases in apoSynCaM18A in comparison with that in apoSynCaM. This agrees with our heat capacity data for the native state of SynCaM mutants (Table 1); the smaller is ΔT_t, the smaller is the partial heat capacity and, consequently, the level of structural flexibility. In 10 mM buffer, the ΔT_t values are somewhat different, which demonstrates the different influence of cacodylate buffer molarity on the thermostability of the lobes.

Temperature Dependence of the Transition Enthalpy. Analysis of Table 1 data for C-terminal and N-terminal lobe melting shows that the transition temperature change due to the mutations is accompanied by a change in corresponding transition enthalpy values. To find out whether there are unambiguous correlations between these parameters, we plotted the transition enthalpies versus T_t for apoSynCaM and its mutants melting in 50 mM buffer (Figure 4). Similar dependencies were obtained for calmodulins melting in 10 mM buffer (data not shown). The points for all proteins

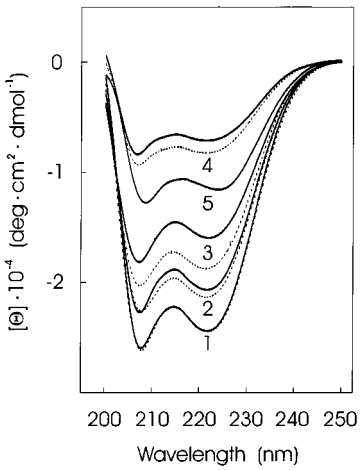

FIGURE 5: CD spectra of SynCaM8 (1), SynCaM (2), SynCaM12A (3), and SynCaM18A (4) in the far-UV region in 50 mM sodium cacodylate buffer at pH 7.5 and CD spectrum of SynCaM (5) in 50 mM HEPES buffer at pH 7.5: (solid lines) apoSynCaMs and (dotted lines) in the presence of 1 mM calcium chloride.

(except the second transition for SynCaM18A) fit two straight lines corresponding to two transitions. These demonstrate that the electrostatic mutations influence the parameters of thermal denaturation of apoSynCaMs in a similar way as pH conditions affect thermal transitions parameters of multidomain proteins (Privalov, 1982; Ruiz-Arribas et al., 1994).

The fact that temperature dependence of the enthalpy for the first transition (Figure 4), that is for the C-terminal lobe, is the same for all calmodulins suggests that the globular structure of this part should be the same for apoSynCaM and its mutants. The analogous conclusion can be drawn for the N-terminal lobe of SynCaM, SynCaM8, and SynCaM12A (Figure 4). The second transition enthalpy value for apoSynCaM18A is considerably lower than is expected for the second transition temperature which is close to that for apoSynCaM (Figure 4). From this fact, we conclude that one domain of the N-terminal lobe of apoSynCaM18A has a folded structure similar to that in apoSynCaM, whereas the other domain is unfolded (fully or partially) in the native state. This agrees with our data on the flexibility increase for the SynCaM18A mutant in comparison to that for SynCaM (Table 1). Thus, the redistribution of charges in the C-terminal lobe and central helix of apoSynCaM results in essential conformational changes in the N-terminal lobe despite the absence of stable, direct contacts between the two lobes in the apoCaM molecule (Kuboniwa et al., 1995).

Circular Dichroism Spectra of SynCaMs. The far-UV CD spectra of SynCaM and its mutants (calcium-free and in the presence of 1 mM calcium chloride) in 50 mM cacodylate buffer at pH 7.5 are shown in Figure 5. Since cacodylate strongly absorbs at the wavelengths below 200 nm, we recorded CD spectra in the wavelength interval 200−250 nm. The general appearance of the far-UV CD spectra of all SynCaMs is similar and of the α-helical type with two minima at about 208 and 222 nm. Analogous CD spectra of SynCaM and SynCaM8 at pH 7.0 were obtained by Craig et al. (1987). As is seen from Figure 5, Ca^{2+} addition has a small effect on the CD spectra of SynCaM, SynCaM8, and SynCaM18A. Only for SynCaM12A does addition of calcium result in a noticeable increase of CD bands.

Table 2: Estimation of the α-Helical Content f_H of SynCaM and Its Mutants from $[\Theta]_{222}$[a–c]

	f_H in 50 mM buffer		f_H in 10 mM buffer	
protein	Ca^{2+}-free	Ca^{2+}-saturated	Ca^{2+}-free	Ca^{2+}-saturated
SynCaM	0.60 (0.30[d])	0.63	0.40 (0.32[d])	0.45
SynCaM8	0.72	0.73	0.50	0.50
SynCaM12A	0.45	0.54	0.32	0.38
SynCaM18A	0.16	0.19	0.28	0.23

[a] Sodium cacodylate buffer at pH 7.5. [b] The calculations in this work were based on the equation $f_H = -([\Theta]_{222} + 2340)/30300$ (Chen et al., 1972). [c] Errors are ±5%. [d] The α-helical content of Ca^{2+}-free SynCaM in HEPES buffer at pH 7.5.

The magnitudes of the CD spectra extrema allow us to conclude that there is a high content of α-helices in all calmodulins studied, except for SynCaM18A. The ellipticity of a polypeptide chain at 222 nm is usually considered an index of its secondary structure (Chen et al., 1972), and the precision of the absolute estimation of helicity from CD is about 5% for proteins with high helical content (Bayley & Martin, 1992). In accordance with this approach, we have estimated the α-helix amount in SynCaMs (Table 2). The highest percent of α-helix was found in 50 mM buffer in SynCaM8 (72−73%) and in SynCaM (60−63%). These may be compared with the value of 63% assessed from the 1.7 Å X-ray crystal structure of Ca^{2+}-CaM (Chattopadhyaya et al., 1992). Essentially lower α-helical content was found in apoSynCaM18A (16% in 50 mM buffer), and addition of calcium increased this value to 19%. Calcium reduces the difference in the α-helical content between SynCaM and its mutants SynCaM8 and SynCaM12A (Table 2). The results obtained show that the replacement of acidic amino acids cluster 82−84 by basic amino acids in SynCaM results in an increased helix content, whereas the replacement of another acidic cluster 118−120 decreases it. However, simultaneous replacement of both clusters in SynCaM does not lead to a compensation of their effects on the helicity but, on the contrary, decreases it more than 3-fold. Therefore, we see from CD data that mutations have a very strong effect on the α-helix and no additivity of the CD effect is observed in the case of simultaneous replacement of two acidic clusters by the basic ones.

It is necessary to note that an absolute CD value at 222 nm is due to both the total α-helical content in the protein and the α-helix distortions (Manning et al., 1988). Most likely, the mutations result in both the α-helical content alteration and geometric distortions within regular α-helices in CaMs. According to Heidorn and Trewhella (1988), the central α-helix of CaM (residues 65−92) could be easily distorted.

Whereas calcium addition has a relatively small effect on the calmodulin secondary structure, the cacodylate buffer molarity, on the contrary, influences it rather appreciably (Table 2). For SynCaM, SynCaM8, and SynCaM12A, the α-helical content is significantly higher in 50 mM buffer solution than in the 10 mM one. These results clearly demonstrate that calmodulins contain regions sensitive to the presence of cacodylate ions which cause an increase of helical conformation. This is also confirmed by the considerable lowering of α-helix content in apoSynCaM on replacing the cacodylate buffer by HEPES (Figure 5, curves 2 and 5; Table 2). Bayley and Martin (1992) have found

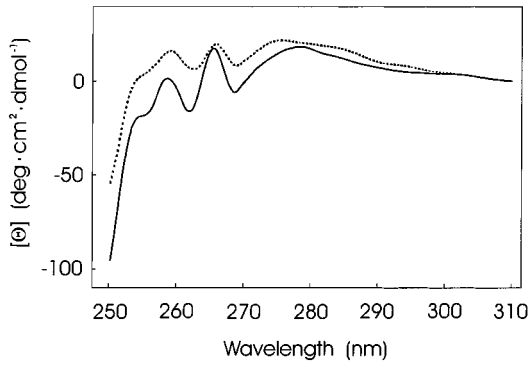

FIGURE 6: CD spectra of apoSynCaM in the near-UV region in 50 mM (solid line) and 10 mM (dotted line) sodium cacodylate buffer at pH 7.5.

that the presence of 2-methyl-2,4-pentanediol (MPD), which is used for CaM crystallization along with cacodylate, also induces additional α-helix in CaM. Our data show that the cacodylate influence on the protein secondary structure is significantly higher than that of MPD. This supports the conclusion made by Bayley and Martin (1992) that the calmodulin conformation contains less α-helix in aqueous solution than is deduced from the crystal structure determined on crystals grown from the mother liquor containing 50 mM cacodylate and MPD (Chattopadhyaya et al., 1992).

The local structure and environment of the side groups of aromatic amino acids can be judged from the near-UV CD. There are no tryptophan residues in the calmodulins studied, and they contain only one C-terminal tyrosine (Tyr138) and nine phenylalanines (Roberts et al., 1985) (Figure 1A,B). Near-UV CD spectra (Figure 6) of all apocalmodulins have identical shapes and, within the limits of experimental error, equal extremum values. Sharp negative CD minima at 262.7 and 269.1 nm characteristic of phenylalanines are seen well; the same two small minima attributed to phenylalanine residues have been found in near-UV CD spectra of ram testis calmodulin (Kilhoffer et al., 1981). The unique tyrosine (Tyr138) exhibits a broad positive CD band near 280 nm (Figure 6).

The X-ray data show that the following α-helical regions are in Ca^{2+}-CaM: residues 5−19, 29−37, and 45−55 in the N-terminal lobe and 102−111, 118−128, and 138−146 in the C-terminal lobe (the helical content of these regions is 44%) and the long central α-helix 65−92 connecting the two lobes (the helical content is 19%) (Chattopadhyaya et al., 1992). Recently, the three-dimensional solution structure of Ca^{2+}-free CaM has been determined by NMR spectroscopy (Kuboniwa et al., 1995), and α-helical regions identical to those found in Chattopadhyaya et al. (1992) were detected. Aromatic amino acid residues in CaMs and SynCaM are present at the same polypeptide chain sites (Kilhoffer et al., 1992a), and all of them (with the exception of Phe99) are located in α-helices 5−19 (Phe12, Phe16, and Phe19) and 138−146 (Tyr138 and Phe141) and at the edges of the central α-helix 65−92 (Phe65, Phe68, Phe89, and Phe92) (Figure 1A,B). The invariability of near-UV CD of all the SynCaMs allows us to conclude that local structure of aromatic residues and local environment of their side groups do not change upon mutations in SynCaM, although secondary structure undergoes significant transformations (Table 2). It can be supposed that in SynCaM18A, characterized by the lowest α-helical content, four α-helical regions free of aromatic residues (29−37, 45−55, 102−111, and 118−128) as well as the central part of α-helix 65−92 are destroyed.

So, the mutations influencing the molecule electrostatic potential cause alterations of SynCaM secondary structure on retention of the protein three-dimensional structure within the regions of aromatic amino acids. Most likely, SynCaM and its mutants differ both in the α-helical content and the level of α-helix distortions. In accordance with the temperature dependence of the transition enthalpy (Figure 4), SynCaM mutants form hydrophobic cores in N-terminal and C-terminal lobes which are similar to those in SynCaM. Hence, changes in the secondary structure not followed by the changes in hydrophobic interactions and near-UV CD spectra bring about the distortion of α-helices rather than the change in their amount. For SynCaM18A, the considerable decrease in the denaturation enthalpy, along with α-helicity (Tables 1 and 2), proves the breakdown of α-helices.

CONCLUSIONS

Calmodulin in the last two decades has appeared as an important protein in the information management of eukaryotic cells. Although we know a lot about its structure, we barely understand its physiological role in the cell. In some way, calmodulin studies illustrate the limits of an extreme reductionism approach.

Calmodulin studies conducted in different laboratories have raised several controversies as some experimental data were somewhat different. A striking illustration of this point is the relative inconsistency between the structural information obtained by X-ray diffraction or NMR and CD. Indeed, the level of α-helix was different when compared. Therefore, calmodulin was considered a "bad" protein that did not follow the regular rules used to interpret the CD spectra. There were some reports incriminating the presence of detergent or a pH difference to explain this inconsistency. In this report, we clearly point out the strong influence of cacodylate molarity on the protein structure. This suggests either an effect of the ionic strength or a more specific effect of the cacodylate ion. We favor the second interpretation as the replacement of cacodylate by HEPES causes the decrease in helical conformation.

The heat denaturation of apoSynCaM is well approximated by two two-state transitions with the lower-temperature transition corresponding to C-terminal lobe melting and the higher-temperature one to N-terminal lobe melting. As was shown by Haiech et al. (1991), the N-terminal lobe of SynCaM has a lower affinity for calcium than the C-terminal lobe. Therefore, our data suggest an inverse relation between the affinity for calcium and thermal stability.

We have shown that the apoSynCaM molecule is more flexible in solution than other small proteins. Replacement of acidic clusters by basic ones in SynCaM demonstrated the role of electrostatic interactions in flexibility and stabilization of this protein. The flexibility of apoSynCaM does not change upon cluster mutation in the C-terminal lobe and decreases for cluster mutation in the central α-helix, which supports its responsibility for the flexibility of the molecule. Simultaneous replacement of both clusters, in mutant SynCaM18A, leads to the significant increase of calmodulin flexibility. Analyzing the melting parameters for SynCaM18A and its CD spectra, we have concluded that

one domain of the N-terminal lobe is unfolded in the native state. This explains the highest flexibility and the lowest α-helical content for this mutant.

Thus, the redistribution of charges in the C-terminal lobe and central helix of apoSynCaM leads to the essential conformational changes in the N-terminal lobe despite the absence of stable, direct contacts between the two lobes in the apoCaM molecule that was shown by NMR (Kuboniwa et al., 1995). Our data unambiguously demonstrate that the two lobes are not independent and interactions between the lobes are mediated by the electrostatic potential of the molecule. The dramatic effect observed with the double mutant SynCaM18A pinpoints the long range effect of electrostatic mutations on the conformation of the whole molecule.

REFERENCES

Afshar, M., Caves, L., Guimard, L., Hubbard, R., Calas, B., Grassy, G., & Haiech, J. (1994) *J. Mol. Biol. 244*, 554−571.

Babu, Y. S., Sack, J. S., Greenhough, T. J., Bugg, C. E., Means, A. R., & Cook, W. J. (1985) *Nature 315*, 37−40.

Bayley, P. M., & Martin, S. R. (1992) *Biochim. Biophys. Acta 1160*, 16−21.

Chattopadhyaya, R., Meador, W. E., Means, A. R., & Quiocho, F. A. (1992) *J. Mol. Biol. 228*, 1177−1192.

Chazin, W. J. (1995) *Nat. Struct. Biol. 2*, 707−710.

Chen, Y. H., Yang, J. T., & Martinez, H. M. (1972) *Biochemistry 11*, 4120−4131.

Craig, T. A., Watterson, D. M., Prendergast, F. G., Haiech, J., & Roberts, D. M. (1987) *J. Biol. Chem. 262*, 3278−3284.

Falke, J. J., Drake, S. K., Hazard, A. L., & Peersen, O. B. (1994) *Q. Rev. Biophys. 27*, 219−290.

Farrar, Y., Lukas, T., Craig, T., Watterson, D. M., & Carlson, G. (1993) *J. Biol. Chem. 268*, 4120−4125.

Filimonov, V. V., Potekhin, S. A., Matveyev, S. V., & Privalov, P. L. (1982) *Mol. Biol. (Moscow) 16*, 435−444.

Filimonov, V. V., Prieto, J., Martinez, J. C., Bruix, M., Mateo, P. L., & Serrano, L. (1993) *Biochemistry 32*, 12906−12921.

Freire, E., & Biltonen, R. L. (1978) *Biopolymers 17*, 463−479.

Haiech, J., Klee, C. B., & Demaille, J. G. (1981) *Biochemistry 20*, 3890−3897.

Haiech, J., Kilhoffer, M.-C., Lukas, T. J., Craig, T. A., Roberts, D. M., & Watterson, D. M. (1991) *J. Biol. Chem. 25*, 3427−3431.

Heidorn, D. B., & Trewhella, J. (1988) *Biochemistry 27*, 909−915.

Hopkins, H. P., & Gayden, R. H. (1990) *J. Phys. Chem. 94*, 7923−7927.

Kilhoffer, M.-C., Demaille, J. G., & Gerard, D. (1981) *Biochemistry 20*, 4407−4414.

Kilhoffer, M.-C., Lukas, T. J., Watterson, D. M., & Haiech, J. (1992a) *Biochim. Biophys. Acta 1160*, 8−15.

Kilhoffer, M.-C., Kubina, M., Travers, F., & Haiech, J. (1992b) *Biochemistry 31*, 8098−8106.

Kosk-Kosicka, D., & Bzdega, T. (1991) *Biochemistry 30*, 65−70.

Kuboniwa, H., Tjandra, N., Grzesiek, S., Ren, H., Klee, C. B., & Bax, A. (1995) *Nat. Struct. Biol. 2*, 768−776.

Kyte, J., & Doolitle, R. F. (1982) *J. Mol. Biol. 157*, 105−132.

Lafitte, D., Capony, J. P., Grassy, G., Haiech, J., & Calas, B. (1995) *Biochemistry 34*, 13825−13832.

Lafitte, D., Gilli, R., Calas, B., Kilhoffer, M.-C., Briand, C., & Haiech, J. (1996) *J. Am. Chem. Soc.* (submitted for publication).

Linse, S., Helmersson, A., & Forsen, S. (1991) *J. Biol. Chem. 266*, 8050−8054.

Makhatadze, G. I., & Privalov, P. L. (1990) *J. Mol. Biol. 213*, 375−384.

Manning, M. C., Illangasekare, M., & Woody, R. W. (1988) *Biophys. Chem. 31*, 77−86.

Massom, L. R., Lukas, T. J., Persechini, A., Kretsinger, R. H., Watterson, D. M., & Jarrett, H. W. (1991) *Biochemistry 30*, 663−667.

Milos, M., Comte, M., Schaer, J. J., & Cox, J. A. (1989) *J. Inorg. Biochem. 36*, 11−25.

Pedigo, S., & Shea, M. A. (1995a) *Biochemistry 34*, 1179−1196.

Pedigo, S., & Shea, M. A. (1995b) *Biochemistry 34*, 10676−10689.

Porumb, T. (1994) *Anal. Biochem. 220*, 227−237.

Privalov, P. L. (1982) *Adv. Protein Chem. 35*, 1−104.

Privalov, P. L., & Potekhin, S. A. (1986) *Methods Enzymol. 131*, 4−51.

Privalov, P. L., & Makhatadze, G. I. (1990) *J. Mol. Biol. 213*, 385−391.

Roberts, D. M., Crea, R., Malecha, M., Alvarado-Urbina, G., Chiarello, R. H., & Watterson, D. M. (1985) *Biochemistry 24*, 5090−5098.

Ruiz-Arribas, A., Santamaria, R. I., Zhadan, G. G., Villar, E., & Shnyrov, V. L. (1994) *Biochemistry 33*, 13787−13791.

Schippers, P. H., & Dekkers, H. P. J. M. (1981) *Anal. Chem. 53*, 778−788.

Serrano, L., Day, A. G., & Fersht, A. R. (1993) *J. Mol. Biol. 233*, 305−312.

Shoemaker, M. O., Lau, W., Shattuck, R. L., Kwiatkowski, A. P., Matrisian, P. E., Guerra-Santos, L., Wilson, E., Lukas, T. J., Van Eldik, L. J., & Watterson, D. M. (1990) *J. Cell Biol. 111*, 1107−1125.

Takakuwa, T., Konno, T., & Meguro, H. (1985) *Anal. Sci. 1*, 215−225.

Tsalkova, T. N., & Privalov, P. L. (1985) *J. Mol. Biol. 181*, 533−544.

Wang, C. L. A. (1985) *Biochem. Biophys. Res. Commun. 130*, 426−430.

Weber, P. C., Lukas, T. J., Craig, T. A., Wilson, E., King, M. M., Kwiatkowski, A. P., & Watterson, D. M. (1989) *Proteins 6*, 70−85.

Zhang, M., Tanaka, T., & Ikura, M. (1995) *Nat. Struct. Biol. 2*, 758−765.

BI962538G